FT-IR and FT-Raman vibrational analysis, ab initio HF and DFT simulations of isocyanic acid 1-naphthyl ester

ARTICLE *in* SPECTROCHIMICA ACTA PART A MOLECULAR AND BIOMOLECULAR SPECTROSCOPY · JUNE 2011

Impact Factor: 2.35 · DOI: 10.1016/j.saa.2011.06.044 · Source: PubMed

4 AUTHORS, INCLUDING:

Mehmet Karabacak
Celal Bayar Üniversitesi
131 PUBLICATIONS **1,476** CITATIONS
SEE PROFILE

Sengeny Periandy
Independent Researcher
82 PUBLICATIONS **683** CITATIONS
SEE PROFILE

S. Ramalingam
A.V.C. College (Autonomous)
71 PUBLICATIONS **383** CITATIONS
SEE PROFILE

Spectrochimica Acta Part A 81 (2011) 504–518

Contents lists available at ScienceDirect

Spectrochimica Acta Part A: Molecular and Biomolecular Spectroscopy

journal homepage: www.elsevier.com/locate/saa

FT-IR and FT-Raman vibrational analysis, ab initio HF and DFT simulations of isocyanic acid 1-naphthyl ester

D. Shoba [a], M. Karabacak [b], S. Periandy [c], S. Ramalingam [d,*]

[a] Department of Physics, Alpha College of Engineering & Technology, Puducherry, India
[b] Department of Physics, Afyon Kocatepe University, Afyonkarahisar, Turkey
[c] Department of Physics, Tagore Arts College, Puducherry, India
[d] Department of Physics, A.V.C. College, Mayiladuthurai, Tamilnadu, India

ARTICLE INFO

Article history:
Received 1 June 2011
Received in revised form 14 June 2011
Accepted 19 June 2011

Keywords:
Isocyanic acid 1-naphthyl ester
HF and DFT
Isocyanato group
HOMO–LUMO

ABSTRACT

The Fourier transform infrared and Fourier transform Raman spectra of isocyanic acid 1-naphthyl ester ($C_{11}H_7NO$) [ICANE] are recorded in solid phase, the harmonic vibrational frequencies, infrared intensities, Raman activities, bond length, bond angle and dihedral angle are calculated by HF and DFT methods by using different basis set. A detailed vibrational spectral analysis has been carried out and assignments of observed fundamental bands have been proposed on basis of peak positions and relative intensities. The scaled theoretical frequencies showed very good agreement with experimental values. A detailed interpretations of the infrared and Raman spectra of isocyanic acid 1-naphthyl ester are reported, the theoretical spectra for infrared and Raman spectrum of title molecule have been constructed. The effect due to the substitutions of isocyanato group is also investigated. A study on the electronic properties, such as excitation energies and wavelengths, are performed with different solvent by time-dependent DFT (TD-DFT) approach. HOMO and LUMO energies are calculated that these energies show charge transfer occurs within the molecule.

1. Introduction

Framework for most of dyes is aromatic rings. Because of the functional group present in it, the dyes owes their colour especially naphthalene plays important role in this field besides it is also a valuable insecticide [1]. Naphthalene and its derivatives are pharmaceutically, biologically and industrially useful compounds. The structure of naphthalene is, like benzene, having two to six membered rings fused together. Especially, naphthalene was studied because of its technological applications in a vast amount of industrial process [2].

Extensive experimental and theoretical investigations have focused on elucidating the structure and normal vibrations of naphthalene and its derivatives. Xavier et al. [3] investigated the methoxynapthalene by using Wilson's F-G matrix method. Dimethylnaphthalenes in the gas phase is studied by Das et al. [4]. Nagabalasubramanian et al. [5] studied the FT-IR and FT-Raman vibrational spectra of 1,5-methylnaphthalene molecule. FT-IR and FT-Raman spectra of 1-methoxynapthalene are reported by Govindarajan et al. [6]. Molecular structure, vibrational spectroscopic, first-order hyperpolarizability and HOMO, LUMO studies of 3-hydroxy-2-naphthoic acid hydrazide are studied [7]. Krishnakumar et al. [1] evaluated structure and vibrational frequencies of 1-naphthaldehyde based on density functional theory calculations. 1-Naphthyl acetic acid is investigated in polycrystalline sample by Fourier transform infrared (FT-IR) and FT-Raman spectroscopy [8].

Liebig and Wöhler [9] first reported on the preparation of isocyanic acid, which later was improved by Baeyer [10]. The preparation and properties of isocyanic acid (formula is HNCO) and some of its derivatives have been described in the literature [11–14]. The polymerization of HNCO leads to a mixture of cyanuric acid (trimer of HNCO) and cyamelide [11,15,16]. Cyanuric acid is a commercially available substance [11,17]. However, there has been some doubt regarding the thermal stability of HNCO and possible formation of dimers or other oligomers with the formula $(HNCO)_n$ [18–20].

At sufficiently high concentrations, isocyanic acid oligomerizes to give cyanuric acid and cyamelide, a polymer. These species usually are easily separated from liquid-phase or gas-phase reaction products. Dilute solutions of isocyanic acid are stable in inert solvents, e.g. ether and chlorinated hydrocarbons. Isocyanic acid 1-naphthyl ester (abbreviation as ICANE) is also known 1-isocyanato-naphthalene is substituted naphthalene with a different functional group that an isocyanato (N=C=O) group attached to a planar naphthalene ring. Literature survey reveals that to the best

* Corresponding author. Tel.: +91 9003398477; fax: +91 9003398477.
E-mail address: ramalingam.physics@gmail.com (S. Ramalingam).

1386-1425/$ – see front matter
doi:10.1016/j.saa.2011.06.044

of our knowledge, no experimental and theoretical electronic and vibrational analysis for ICANE molecule has been performed yet. This inadequacy observed in the literature encouraged us to make this theoretical and experimental research to give a correct assignment of the fundamental modes and electronic properties of ICANE in optimum energy conformation and analyze the influences of isocyanato group on the geometry, vibrational spectra and electronic system.

2. Experimental details

The compound under investigation namely isocyanic acid 1-naphthyl ester is purchased from Sigma–Aldrich Chemicals, U.S.A. which is of spectroscopic grade and hence used for recording the spectra as such without any further purification. The FT-IR spectra of the compounds are recorded in Bruker IFS 66V spectrometer in the range of 3600–100 cm^{-1}. The spectral resolution is $\pm 2\,cm^{-1}$. The FT-Raman spectra of these compounds are also recorded in the same instrument with FRA 106 Raman module equipped with Nd:YAG laser source operating at 1.064 μm line widths with 200 mW power. The spectra are recorded in the range of 3600–100 cm^{-1} min^{-1} of spectral width 2 cm^{-1}. The frequencies of all sharp bands are accurate to $\pm 1\,cm^{-1}$.

3. Computational methods

The entire calculation are performed at Hartree–Fock (HF), LSDA, B3LYP levels on Pentium IV personal computer using Gaussian 03 program package, involving gradient geometry optimization [21–23] initial geometry generated standard geometrical parameters minimized without any constraint in the potential energy surface at Hartree–Fock level, adopting the 3-21+G, 6-31+G(d,p) and 6-311+G(d,p) basis sets. This geometry is then re-optimized again at LSDA and B3LYP levels, using the basis set 3-21+G, 6-31+G(d,p) and 6-311+G(d,p).

The optimized structural parameters are used in the vibrational frequency calculation at HF and DFT levels, to characterize all stationary points. Vibrational frequencies are scaled by 0.905, 0.885, 0.929, 0.805, 1.177 for HF/3-21+G, HF/6-31+G(d,p) is scaled by 0.905, 0.879, 0.935, 0.955 and 1.385, HF/6-311+G(d,p) is scaled with 0.911, 0.885, 0.961, 0.921 and 1.395. LSDA/3-21+G basis set is scaled

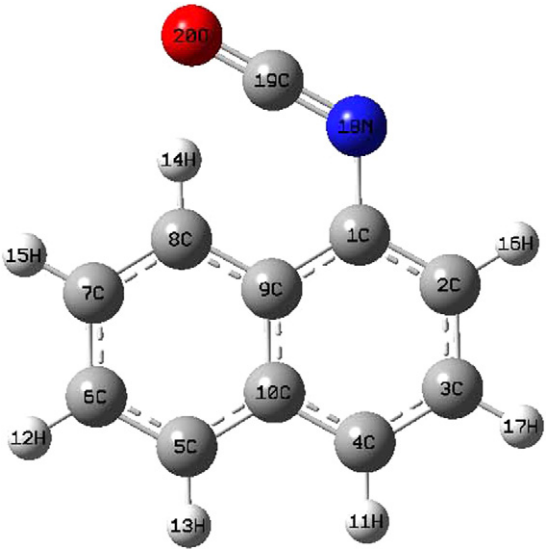

Fig. 1. Molecular structure of isocyanic acid 1-naphthyl ester.

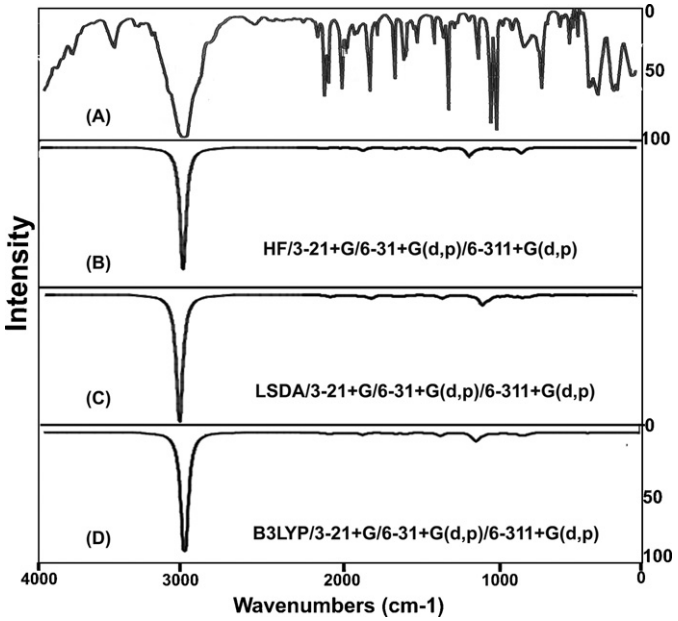

Fig. 2. Experimental [A], calculated [B], [C] and [D] FTIR spectra of isocyanic acid 1-naphthyl ester.

by 0.978, 0.964, 1.039, 0.854, and 1.301, LSDA/6-31+G(d,p) is scaled using 0.978, 0.954, 1.045 and 1.491, LSDA/6-311+G(d,p) scaled by 0.988, 0.959, 1.025, 1.073 and 1.489. B3LYP/3-21+G is scaled with 0.955, 0.935, 1.011, 0.851 and 1.295, B3LYP/6-31+G(d,p) is scaled using 0.956, 0.940, 0.985, 1.030 and 1.456 and B3LYP/6-311+G(d,p) basis set is scaled with 0.970, 0.945, 1.025 and 1.465. By combining the results of Gauss view program with symmetry considerations, vibrational frequency assignments are made with a high degree of accuracy. In order to fit the theoretical wave number to the experimental wave numbers an overall scaling factor has been introduced by using a least square optimization of the computed to the experimental data.

The changes in the thermodynamic functions the heat capacity, entropy, and enthalpy are investigated for the different temperatures from the vibrational frequencies calculations of title molecule. In addition, to calculate the excitation energies of the title molecule, TD-DFT calculations started from gas phase and solution phase optimized geometries are carried out using B3LYP/6-311+G(d,p).

4. Results and discussion

4.1. Molecular geometry

The molecular structure of ICANE belongs to Cs point group symmetry. The optimized molecular structure of title molecule is obtained from Gaussian 09 and Gaussview 05 program and they are shown in Fig. 1. The molecule contain C=O and C=N (isocyanato (N=C=O) group) connected with naphthalene ring. The structure optimization and zero point vibrational energy of title compound in HF/3-21+G/6-31+G/6-311+G(d,p), LSDA/3-21+G/6-31/6-311+G(d,p) and B3LYP/3-21+G/6-31/6-311+G(d,p) are 431988.3, 423260.7, 421284.5, 395400.6, 388292.7, 387227.9, 402882.6, 395487.0, 394322.0 J/M^{-1} and 103.24767, 101.16173, 100.68940, 94.50302, 92.80419, 92.54968, 96.29125, 94.52367, 94.24521 kcal M^{-1}, respectively. The biggest and smallest values of ZPVE of ICANE are obtained by HF/3-21+G* and LSDA/6-311+G(d,p), respectively.

Dipole moment describes the molecular charge distribution and is given as a vector in three dimensions. Therefore, it can be used

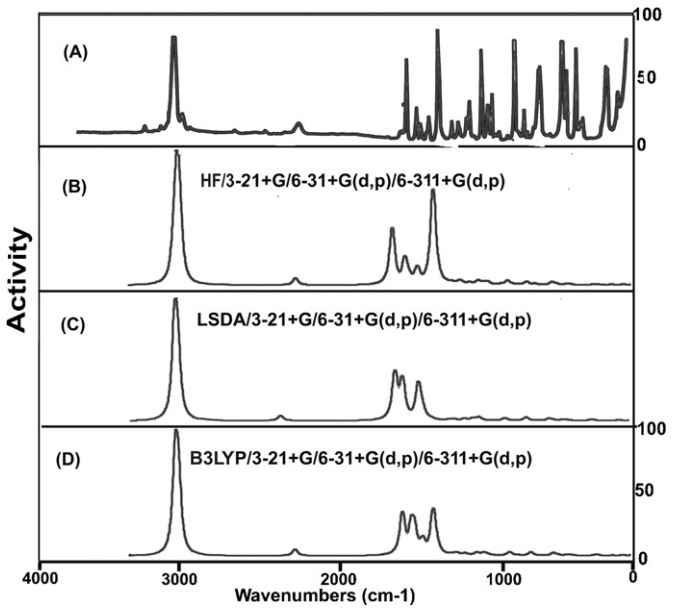

Fig. 3. Experimental [A], calculated [B], [C] and [D] FT Raman spectra of isocyanic acid 1-naphthyl ester.

as descriptor to show the charge movement across the molecule. Direction of the dipole moment vector in a molecule depends on the centers of negative and positive charges. For charged systems, its value depends on the choice of origin and molecular orientation. As a result of HF and DFT (LSDA and B3LYP) calculations the highest dipole moment is observed for HF/3-21G+* whereas the smallest one is observed for LSDA/6-311++G(d,p) in title molecule (see Table 1). The comparative graph of experimental and simulated spectra of IR and Raman are presented in Figs. 2 and 3 respectively.

The comparative optimized structural parameters such as bond lengths bond angles and dihedral angle are presented in Table 2 along with available experimental data. Unlike benzene, the carbon–carbon bonds in naphthalene are not of the same length. The bonds, C1–C2, C3–C4, C5–C6, C7–C8 are ca. 1.36 Å, where as the other carbon bands are like C2–C3, C4–C10, C5–C10, C6–C7, C9–C10, C8–C9 ca. 1.42 Å in HF/3-21+G and HF/6-31/6-311+G(d,p) basis set this difference, which was established by X-ray diffraction is consistent with the valence bond model of bonding in naph-

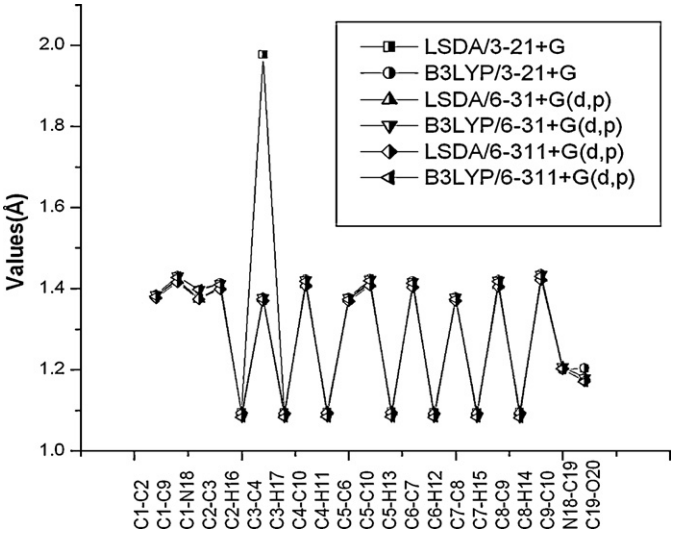

Fig. 4. Bond length differences between theoretical approaches.

Table 1
The calculated thermo dynamical parameters of isocyanic acid 1-naphthyl ester molecule in ground state at 298.15 K.

Basic set	HF3-21+G*	HF6-31+G(d,p)	HF6-311+G(d,p)	LSDA3-21+G*	LSDA6-31+G(d,p)	LSDA6-311+G(d,p)	B3LYP3-21+G*	B3LYP6-31+G(d,p)	B3LYP6-311+G(d,p)
SCF energy (a.u.)	−546.9427	−549.9855	−550.0849	−547.3247	−550.3085	−550.4270	−550.3927	−553.4068	−553.5208
Zero point vib. energy (kcal M^{-1})	103.247	101.161	100.689	94.503	92.804	92.549	96.291	94.523	94.245
Rotational constants (GHz)	1.37953	1.51295	1.52958	1.43518	1.47978	1.50205	1.43445	1.49021	1.50354
	0.62473	0.59938	0.60023	0.60198	0.59981	0.60187	0.59232	0.58921	0.59132
	0.43000	0.42931	0.43107	0.42410	0.42681	0.42969	0.41921	0.42225	0.42441
Specific heat (C_v) (cal mol^{-1} K^{-1})	33.415	35.129	35.173	37.249	39.128	39.067	36.384	38.157	38.137
Entropy (S) (cal mol^{-1} K^{-1})	93.827	96.741	96.793	96.174	98.721	98.854	95.546	97.952	98.140
Dipole moment μ (Debye)	4.3116	2.7887	2.6120	3.2624	2.5328	2.3864	3.5656	2.6567	2.5480

Table 2
Optimized geometrical parameters for isocyanic acid 1-naphthyl ester computed at HF/3-21/6-31/6-311+G(d,p), LSDA/3-21/6-31/6-311+G(d,p) and B3LYP/3-21/6-31/6-311+G(d,p) basis sets.

S. no.	Geometrical parameters	Methods								
		HF			LSDA			B3LYP		
		3-21+G	6-31+G(d,p)	6-311+G(d,p)	3-21+G	6-31+G(d,p)	6-311+G(d,p)	3-21+G	6-31+G(d,p)	6-311+G(d,p)
Bond lengths (Å)										
1	C1–C2	1.362	1.362	1.360	1.383	1.382	1.377	1.385	1.384	1.380
2	C1–C9	1.425	1.426	1.425	1.422	1.420	1.416	1.431	1.430	1.428
3	C1–N18	1.387	1.399	1.402	1.375	1.374	1.374	1.397	1.398	1.398
4	C2–C3	1.411	1.413	1.413	1.406	1.403	1.399	1.414	1.412	1.410
5	C2–H16	1.071	1.075	1.075	1.095	1.095	1.093	1.084	1.085	1.084
6	C3–C4	1.359	1.359	1.356	1.377	1.375	1.370	1.378	1.378	1.374
7	C3–H17	1.072	1.075	1.075	1.095	1.095	1.093	1.084	1.085	1.083
8	C4–C10	1.41	1.420	1.419	1.413	1.411	1.407	1.423	1.421	1.418
9	C4–H11	1.073	1.075	1.075	1.096	1.096	1.094	1.085	1.086	1.084
10	C5–C6	1.359	1.359	1.357	1.376	1.374	1.369	1.378	1.377	1.373
11	C5–C10	1.419	1.421	1.420	1.414	1.411	1.408	1.424	1.422	1.420
12	C5–H13	1.073	1.075	1.075	1.097	1.096	1.094	1.086	1.086	1.084
13	C6–C7	1.415	1.416	1.415	1.411	1.408	1.404	1.419	1.417	1.414
14	C6–H12	1.072	1.075	1.075	1.095	1.095	1.093	1.085	1.086	1.084
15	C7–C8	1.360	1.360	1.358	1.376	1.375	1.370	1.379	1.378	1.374
16	C7–H15	1.072	1.075	1.075	1.095	1.095	1.093	1.085	1.086	1.084
17	C8–C9	1.418	1.420	1.419	1.410	1.408	1.404	1.421	1.420	1.418
18	C8–H14	1.071	1.073	1.072	1.096	1.096	1.094	1.084	1.084	1.082
19	C9–C10	1.41	1.410	1.408	1.429	1.426	1.422	1.435	1.433	1.430
20	N18–C19	1.165	1.185	1.184	1.200	1.206	1.202	1.198	1.207	1.202
21	C19–O20	1.186	1.153	1.144	1.202	1.181	1.171	1.204	1.179	1.170
Bond angle (°)										
1	C2–C1–C9	121.0	120.9	120.8	120.6	120.6	120.5	120.9	120.8	120.7
2	C2–C1–N18	120.2	121.6	121.7	121.5	121.7	121.8	121.1	121.6	121.6
3	C9–C1–N18	118.6	117.3	117.3	117.8	117.5	117.6	117.9	117.5	117.6
4	C1–C2–C3	120.1	120.1	120.2	120.2	120.1	120.22	120.2	120.2	120.3
5	C1–C2–H16	119.7	120.1	120.1	119.4	119.2	119.2	119.7	119.6	119.6
6	C3–C2–H16	120.0	119.6	119.6	120.3	120.5	120.4	119.9	120.0	119.9
7	C2–C3–C4	120.3	120.5	120.5	120.5	120.6	120.7	120.5	120.6	120.6
8	C2–C3–H17	119.0	119.0	118.9	119.1	119.1	119.0	119.0	119.0	119.0
9	C4–C3–H17	120.5	120.4	120.4	120.2	120.1	120.2	120.4	120.2	120.3
10	C3–C4–C10	120.5	120.4	120.3	120.5	120.4	120.4	120.6	120.5	120.5
11	C3–C4–H11	120.6	120.5	120.5	120.7	120.7	120.7	120.5	120.4	120.5
12	C10–C4–H11	118.8	119.0	119.0	118.7	118.7	118.7	118.8	118.9	118.9
13	C6–C5–C10	120.8	120.8	120.8	120.8	120.9	120.9	120.9	120.9	120.9
14	C6–C5–H13	120.5	120.4	120.4	120.7	120.6	120.7	120.5	120.4	120.4
15	C10–C5–H13	118.5	118.4	118.7	118.4	118.3	118.3	118.5	118.5	118.5
16	C5–C6–C7	120.1	120.1	120.1	120.2	120.2	120.2	120.2	120.1	120.1
17	C5–C6–H12	120.3	120.2	120.2	120.1	120.0	120.0	120.2	120.0	120.1
18	C7–C6–H12	119.5	119.6	119.6	119.6	119.7	119.6	119.5	119.7	119.6
19	C6–C7–C8	120.4	120.4	120.4	120.3	120.3	120.3	120.4	120.4	120.4
20	C6–C7–H15	119.4	119.5	119.5	119.5	119.7	119.7	119.4	119.6	119.6
21	C8–C7–H15	120.0	119.9	120.0	120.0	119.9	119.9	120.0	119.8	119.9
22	C7–C8–C9	120.4	120.4	120.4	120.4	120.4	120.4	120.5	120.5	120.6
23	C7–C8–H14	120.4	120.5	120.5	121.3	121.3	121.3	120.7	120.6	120.6
24	C9–C8–H14	119.0	119.0	118.9	118.2	118.2	118.1	118.7	118.7	118.7
25	C1–C9–C8	122.6	122.4	122.4	121.8	121.8	121.8	122.5	122.5	122.5
26	C1–C9–C10	118.1	118.2	118.3	118.5	118.5	118.6	118.2	118.2	118.3
27	C8–C9–C10	119.2	119.2	119.2	119.5	119.6	119.5	119.2	119.2	119.1
28	C4–C10–C5	121.5	121.5	121.4	122.0	122.0	122.0	121.8	121.8	121.8
29	C4–C10–C9	119.6	119.6	119.6	119.4	119.5	119.4	119.4	119.5	119.5
30	C5–C10–C9	118.8	118.8	118.8	118.4	118.4	118.4	118.6	118.5	118.6
31	C1–N18–C19	169.4	141.4	139.0	153.4	146.0	143.6	151.7	141.7	140.8
32	N18–C19–O20	181.6	184.9	184.8	184.9	186.0	185.9	174.7	186.3	186.0
33	N18–C19–O20	180.0	180.0	180.0	180.0	180.0	180.0	180.0	180.0	180.0
Dihedral angle (°)										
1	C9–C1–C2–C3	0.0	0.0	0.0	0.0	0.0	0.0	0.0	0.0	0.0
2	C9–C1–C2–H16	180.0	180.0	180.0	180.0	180.0	180.0	180.0	180.0	180.0
3	N18–C1–C2–C3	180.0	180.0	180.0	180.0	180.0	180.0	180.0	180.0	180.0
4	N18–C1–C2–H16	0.0	0.0	0.0	0.0	0.0	0.0	0.0	0.0	0.0
5	C2–C1–C9–C8	180.0	180.0	180.0	180.0	180.0	180.0	180.0	180.0	180.0
6	C2–C1–C9–C10	0.0	0.0	0.0	0.0	0.0	0.0	0.0	0.0	0.0
7	N18–C1–C9–C8	0.0	0.0	0.0	0.0	0.0	0.0	0.0	0.0	0.0
8	N18–C1–C9–C10	180.0	180.0	180.0	180.0	180.0	180.0	180.0	180.0	180.0
9	C2–C1–N18–C19	0.0	0.0	0.0	0.0	0.0	0.0	0.0	0.0	0.0
10	C9–C1–N18–C19	180.0	180.0	180.0	180.0	180.0	180.0	180.0	180.0	180.0
11	C1–C2–C3–C4	0.0	0.0	0.0	0.0	0.0	0.0	0.0	0.0	0.0
12	C1–C2–C3–H17	180.0	180.0	180.0	180.0	180.0	180.0	180.0	180.0	180.0
13	H16–C2–C3–C4	180.0	180.0	180.0	180.0	180.0	180.0	180.0	180.0	180.0

Table 2 (*Continued*)

S. no.	Geometrical parameters	Methods								
		HF			LSDA			B3LYP		
		3-21+G	6-31+G(d,p)	6-311+G(d,p)	3-21+G	6-31+G(d,p)	6-311+G(d,p)	3-21+G	6-31+G(d,p)	6-311+G(d,p)
14	H16–C2–C3–H17	0.0	0.0	0.0	0.0	0.0	0.0	0.0	0.0	0.0
15	C2–C3–C4–C10	0.0	0.0	0.0	0.0	0.0	0.0	0.0	0.0	0.0
16	C2–C3–C4–H11	180.0	180.0	180.0	180.0	180.0	180.0	180.0	180.0	180.0
17	H17–C3–C4–C10	180.0	180.0	180.0	180.0	180.0	180.0	180.0	180.0	180.0
18	H17–C3–C4–H11	0.0	0.0	0.0	0.0	0.0	0.0	0.0	0.0	0.0
19	C3–C4–C10–C5	180.0	180.0	180.0	180.0	180.0	180.0	180.0	180.0	180.0
20	C3–C4–C10–C9	0.0	0.0	0.0	0.0	0.0	0.0	0.0	0.0	0.0
21	H11–C4–C10–C5	0.0	0.0	0.0	0.0	0.0	0.0	0.0	0.0	0.0
22	H11–C4–C10–C9	180.0	180.0	180.0	180.0	180.0	180.0	180.0	180.0	180.0
23	C10–C5–C6–C7	0.0	0.0	0.0	0.0	0.0	0.0	0.0	0.0	0.0
24	C10–C5–C6–H12	180.0	180.0	180.0	180.0	180.0	180.0	180.0	180.0	180.0
25	H13–C5–C6–C7	180.0	180.0	180.0	180.0	180.0	180.0	180.0	180.0	180.0
26	H13–C5–C6–H12	0.0	0.0	0.0	0.0	0.0	0.0	0.0	0.0	0.0
27	C6–C5–C10–C4	180.0	180.0	180.0	180.0	180.0	180.0	180.0	180.0	180.0
28	C6–C5–C10–C9	0.0	0.0	0.0	0.0	0.0	0.0	0.0	0.0	0.0
29	H13–C5–C10–C4	0.0	0.0	0.0	0.0	0.0	0.0	0.0	0.0	0.0
30	H13–C5–C10–C9	180.0	180.0	180.0	180.0	180.0	180.0	180.0	180.0	180.0
31	C5–C6–C7–C8	0.0	0.0	0.0	0.0	0.0	0.0	0.0	0.0	0.0
32	C5–C6–C7–H15	180.0	180.0	180.0	180.0	180.0	180.0	180.0	180.0	180.0
33	H12–C6–C7–C8	180.0	180.0	180.0	180.0	180.0	180.0	180.0	180.0	180.0
34	H12–C6–C7–H15	0.0	0.0	0.0	0.0	0.0	0.0	0.0	0.0	0.0
35	C6–C7–C8–C9	0.0	0.0	0.0	0.0	0.0	0.0	0.0	0.0	0.0
36	C6–C7–C8–H14	180.0	180.0	180.0	180.0	180.0	180.0	180.0	180.0	180.0
37	H15–C7–C8–C9	180.0	180.0	180.0	180.0	180.0	180.0	180.0	180.0	180.0
38	H15–C7–C8–H14	0.0	0.0	0.0	0.0	0.0	0.0	0.0	0.0	0.0
39	C7–C8–C9–C1	180.0	180.0	180.0	180.0	180.0	180.0	180.0	180.0	180.0
40	C7–C8–C9–C10	0.0	0.0	0.0	0.0	0.0	0.0	0.0	0.0	0.0
41	H14–C8–C9–C1	0.0	0.0	0.0	0.0	0.0	0.0	0.0	0.0	0.0
42	H14–C8–C9–C10	180.0	180.0	180.0	180.0	180.0	180.0	180.0	180.0	180.0
43	C1–C9–C10–C4	0.0	0.0	0.0	0.0	0.0	0.0	0.0	0.0	0.0
44	C1–C9–C10–C5	180.0	180.0	180.0	180.0	180.0	180.0	180.0	180.0	180.0
45	C8–C9–C10–C4	180.0	180.0	180.0	180.0	180.0	180.0	180.0	180.0	180.0
46	C8–C9–C10–C5	0.0	0.0	0.0	0.0	0.0	0.0	0.0	0.0	0.0

For numbering of atoms refer Fig. 1.

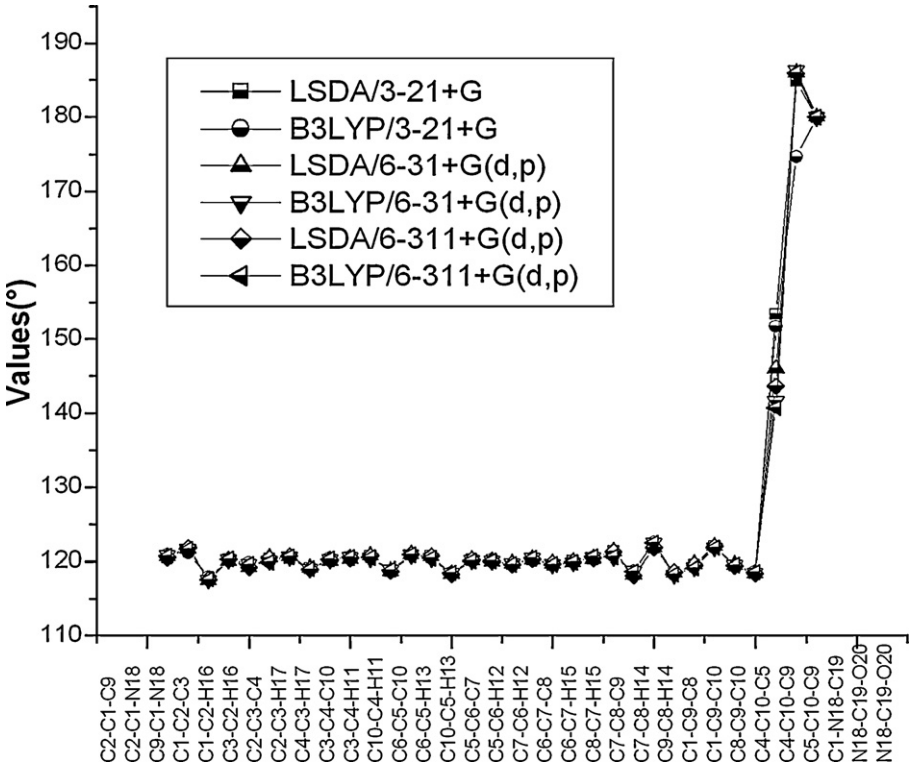

Fig. 5. Bond angle differences between theoretical approaches.

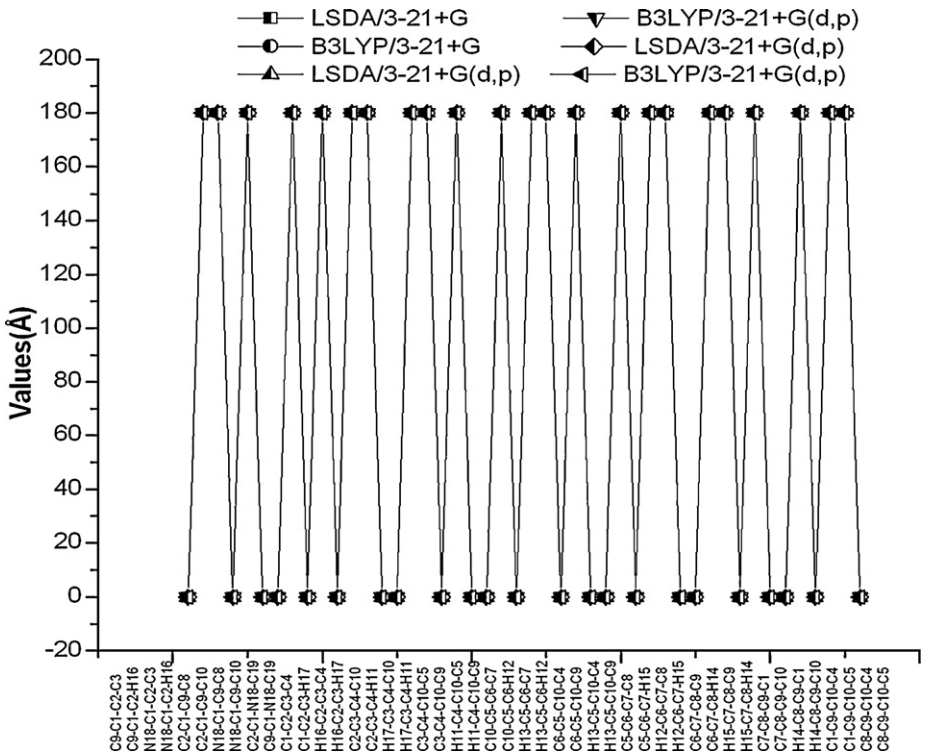

Fig. 6. Dihedral angle differences between theoretical approaches.

thalene that involves the three resonance structures whereas the bonds C1–C2, C3–C4, C5–C6 and C7–C8 are double in two of the three structures, the others are double in only one Jas et al. [24] show that C9–C10, C4–C3, C10–C5 and C2–C3 bond lengths were 1.409, 1.358, 1.421, 1.417, respectively and also the geometrical parameters calculated in the literature [25–27] are very close with our calculated data.

All C–H bond length are 1.073 Å in HF 1.095 Å and 1.080 Å in B3LYP this shows that C–H bond lengths computed with LSDA/3-21+G and LSDA/6-31/6-311+G(d,p) basis sets are closer to the experimental data. Hence the bond lengths calculated by LSDA method are more accurate when compared with experimental values. The HF/3-21+G and HF/6-31/6-311+G(d,p) bond lengths are slightly shorter due to the neglect of electron correlation, while the LSDA basis sets are closer to experimental data due to slightly exaggerated electron correlation effect. N–C and C–O bond length in LSDA and B3LYP is (ca. 0.02 Å) and (ca. 0.03 Å) longer than HF.

The bond angles are calculate using various methods shows the same trends as significant variation in bond lengths. The bond angle (C1–N18–C19) is different with the basis set and N18–C19–O20 bond angle is 180° in all the basis set this shows that substituent isocyanato (N=C=O) group is linear. The other words, the naphthalene ring is planar, and also the isocyanato (N=C=O) group is lying approximately in the plane as evident from the torsional angles by all methods. Exactly at the substitution place the bond angle (C9–C1–C2) 121° rather than the hexagonal angle 120° and also N18–C1–C2 bond angle is 121.8°, C9–C1–N18 is 117°, this shows that the naphthalene ring is little distorted. The comparative graph of bond length, bond angle and dihedral angle are presented in Figs. 4–6 respectively.

4.2. Computed IR intensity and Raman activity analysis

Computed vibrational spectral IR intensities and Raman activities of ICANE molecule for corresponding wave numbers by HF and DFT (LSDA, B3LYP) methods at 3-21+G, 6-31+G(d,p) and 6-311+G(d,p) basis set have been presented in Table 3. Comparison of IR intensities and Raman activities calculated by HF and DFT (B3LYP and LSDA) at different levels with experimental values exposes the variation of IR intensities and Raman activities. In case of IR intensity HF and B3LYP basis sets are higher than LSDA. Whereas most of Raman activities are higher in HF/6-31+G, LSDA/6-31+G and B3LYP/6-31+G(d,p) than HF/6-311+G, LSDA/6-311+G and B3LYP/6-311+G(d,p) basis set. The comparative graph of IR intensities and Raman activities for 5 sets are presented in Figs. 7 and 8. In this present work very high intensities are observed at frequencies 2260, 3060, 1610, 1400, 800, 555 cm^{-1} in HF, LSDA and B3LYP.

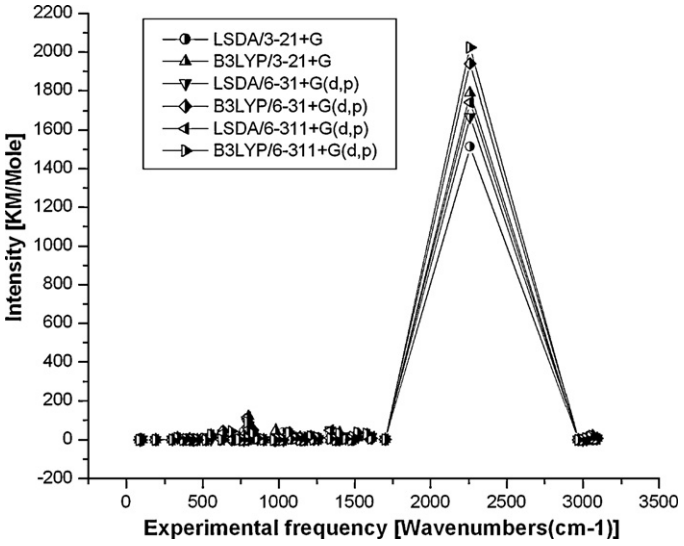

Fig. 7. Comparative graph of IR intensities by DFT [LSDA/B3LYP].

Table 3
Comparative values of IR-intensity and Raman activity between HF/3-21/6-31/6-311+G(d,p), LSDA/3-21/6-31/6-311+G(d,p) and B3LYP/3-21/6-31/6-311+G(d,p) of isocyanic acid 1-naphthyl ester.

S. no.	Calculated with HF						Calculated with LSDA						Calculated with B3LYP					
	3-21+G		6-31+G(d,p)		6-311+G(d,p)		3-21+G		6-31+G(d,p)		6-311+G(d,p)		3-21+G		6-31+G(d,p)		6-311+G(d,p)	
	IR intensity	Raman activity	IR intensity	Raman activity	IR intensity	Raman activity	IR intensity	Raman activity	IR intensity	Raman activity	IR intensity	Raman activity	IR intensity	Raman activity	IR intensity	Raman activity	IR intensity	Raman activity
1	7.7	139.2	6.48	116.9	5.8	112.8	0.93	445.1	6.55	465.0	5.59	398.7	8.44	218.0	8.16	202.5	7.22	201.8
2	9.4	178.0	15.11	249.6	14.7	253.7	11.39	126.0	6.12	156.9	3.38	213.0	12.70	198.0	13.36	237.7	11.95	239.8
3	23.7	166.9	29.58	136.7	28.7	129.8	8.27	67.54	7.91	80.62	6.10	74.16	22.25	153.6	22.89	167.3	20.66	157.3
4	16.4	103.0	22.24	100.1	21.3	105.6	6.16	90.14	7.33	79.46	6.01	73.0	14.22	100.3	16.2	94.64	15.57	92.58
5	8.7	123.9	5.76	103.9	4.8	89.06	1.68	99.92	1.66	99.65	1.84	109	9.73	132.3	9.19	134.9	7.48	128.1
6	0.2	38.9	1.65	26.54	2.9	23.16	0.33	58.38	0.18	58.82	0.00	49.3	0.26	43.92	0.10	43.66	0.19	35.82
7	0.2	33.3	0.36	39.87	0.39	41.14	1.32	54.56	2.05	66.60	0.93	49.94	0.57	40.31	0.70	39.18	0.46	37.46
8	26.8	165.1	2969	40.34	29.9	30.11	1514	85.23	1667	44.25	1742	34.02	1788	101.6	1941	44.11	2024	36.80
9	1.9	1.7	6.05	3.53	6.5	3.34	3.37	3.83	3.45	4.16	3.58	3.99	2.700	4.48	3.15	4.51	3.21	4.23
10	16.1	3.9	20.31	6.96	21.0	5.51	9.76	3.51	16.07	57.80	15.84	35.01	9.35	0.88	8.32	0.80	9.35	1.02
11	16.6	286.2	42.03	259.6	45.8	235.2	17.43	313.0	21.26	287.8	26.36	268.8	19.42	256.3	29.4	252.3	31.33	232.1
12	10.1	32.9	58.60	106.9	73.0	99.34	10.47	235.4	16.61	254.5	24.10	253.1	11.84	51.62	33.5	153.0	37.28	148.9
13	1.1	38.5	7.8	20.4	13.9	23.45	2.99	69.03	4.42	3.79	4.08	3.98	4.85	101.4	12.7	121.7	15.38	113.5
14	1.4	50.0	1.3	12.85	2.3	11.82	1.26	17.05	5.93	224.7	1.79	113.4	6.46	53.93	1.32	16.58	1.13	13.07
15	8.7	45.3	11.1	54.88	9.3	54.63	9.99	110.2	6.34	21.79	10.76	122.8	0.69	115.9	7.27	65.39	6.62	61.91
16	73.0	27.5	38.5	5.22	35.7	4.97	1.81	183.1	2.02	32.02	2.12	39.75	38.50	63.1	27.5	47.32	31.80	14.58
17	1.1	366.3	2.9	399.6	3.1	400.5	16.04	3.95	0.71	11.32	0.06	7.45	1.16	277.3	0.25	215.7	0.64	249.6
18	1.5	7.9	2.6	18.50	1.8	17.89	34.62	15.22	48.98	7.72	49.64	7.77	1.37	7.79	10.3	17.53	6.64	18.44
19	1.6	21.7	10.8	3.73	10.6	3.47	0.60	3.16	5.69	2.54	6.12	2.70	0.82	4.29	9.58	4.49	9.43	4.04
20	12.5	6.6	14.7	8.51	14.7	7.65	8.41	4.67	10.03	6.55	9.34	5.44	10.35	8.19	1.41	6.26	3.11	7.44
21	27.8	4.3	1.1	2.33	1.0	2.21	7.31	5.82	9.82	8.34	9.15	8.08	9.75	7.82	20.2	10.12	18.42	8.37
22	0.1	0.7	0.5	13.40	0.6	13.55	17.94	7.16	0.88	4.55	0.60	3.83	8.11	5.03	0.72	2.87	0.63	3.13
23	3.1	6.9	2.7	3.98	2.6	3.75	7.24	4.34	2.24	0.37	2.81	0.26	4.08	2.44	7.62	5.64	8.61	4.80
24	7.5	3.0	16.5	9.21	15.9	8.53	0.41	2.90	0.59	8.89	0.55	8.71	13.30	9.24	1.33	4.00	1.03	4.17
25	13.0	8.7	8.9	15.77	9.5	15.66	1.64	3.86	9.21	14.69	9.99	14.60	7.75	0.95	7.18	17.37	7.61	17.22
26	0.8	0.1	0.0	2.78	0.0	1.97	8.83	15.98	9.25	22.22	9.63	22.37	7.02	17.19	6.08	16.69	6.42	15.99
27	2.1	1.1	2.2	1.59	32.3	4.53	7.21	19.09	28.93	2.02	28.71	1.83	0.33	0.14	37.2	5.30	37.41	5.75
28	0.9	3.0	30.5	4.89	1.9	1.13	38.31	3.18	0.00	0.46	0.00	0.33	6.92	12.35	0.00	0.73	0.00	0.53
29	9.6	17.9	0.3	4.30	0.16	4.40	0.29	0.09	2.30	0.27	1.93	0.24	1.38	0.97	1.87	0.43	1.67	0.34
30	2.6	4.0	14.40	10.76	11.5	10.98	1.60	0.68	0.31	1.01	0.30	0.92	46.87	6.94	0.27	1.82	0.24	1.66
31	59.4	1.4	0.52	1.16	0.4	1.05	1.38	0.64	0.08	0.20	0.44	0.14	1.09	1.11	0.00	0.46	0.00	0.43
32	9.8	10.4	2.77	3.62	3.0	3.29	0.68	1.10	1.23	0.69	1.24	0.79	0.82	1.71	1.39	1.16	1.60	0.95
33	0.0	0.0	10.05	19.55	9.4	18.01	10.69	19.87	4.10	18.49	4.41	17.0	0.01	0.02	8.32	22.57	8.74	21.67
34	175.	0.11	105.5	2.85	64.2	2.31	0.00	0.01	31.17	1.04	7.03	0.48	19.69	26.26	53.25	1.23	29.62	0.74
35	30.3	24.4	51.31	2.52	78.2	0.74	1.72	3.00	1.71	3.47	1.86	3.13	119.6	0.09	3.20	2.78	3.32	2.62
36	10.0	0.92	6.96	1.59	7.07	1.46	11.2	0.08	89.06	0.10	114.7	0.04	3.35	2.92	65.04	0.32	89.54	0.06
37	7.7	2.0	0.00	1.18	0.08	0.96	41.14	0.36	0.13	0.30	0.00	0.27	25.57	0.78	0.00	0.89	0.04	0.74
38	22.4	0.15	19.38	16.28	32.2	13.74	10.69	0.10	0.76	23.08	0.81	22.5	14.87	0.27	1.12	21.78	2.26	20.86
39	14.9	10.9	62.33	2.79	47.2	5.62	4.69	18.18	0.88	0.07	0.27	0.03	6.15	15.55	0.56	0.12	44.34	1.57
40	28.9	0.3	0.90	0.008	7.1	0.08	19.32	0.12	34.65	2.86	35.96	1.71	17.87	0.19	44.8	1.62	0.10	0.08
41	53.8	2.5	41.94	1.58	33.5	1.16	26.61	6.06	9.21	0.04	2.26	0.12	36.57	4.09	5.69	0.02	2.40	0.48
42	75.5	1.9	14.15	0.03	13.5	0.04	17.96	2.27	0.89	12.24	23.03	1.23	26.29	1.97	24.4	1.47	27.60	0.76
43	2.1	13.9	1.77	11.70	2.0	11.73	3.82	12.28	15.41	1.61	0.39	13.5	2.33	14.42	0.29	13.98	0.24	14.55
44	0.0	0.6	2.54	5.55	2.5	5.41	0.73	5.96	0.82	5.17	0.79	5.06	1.38	6.52	1.29	5.51	1.37	5.50
45	1.3	7.7	0.18	0.22	0.1	0.36	0.15	0.16	0.00	0.05	0.00	0.07	0.04	0.33	0.04	0.12	0.03	0.15
46	0.0	4.2	3.29	3.30	3.3	3.13	0.24	7.76	1.06	7.54	1.19	7.29	0.43	6.70	1.26	6.49	1.31	6.32
47	8.9	2.2	5.16	1.57	5.1	1.37	8.03	0.81	0.65	5.04	0.61	4.94	6.41	1.01	0.42	4.24	0.39	4.07
48	0.7	3.2	0.90	3.64	0.7	3.62	0.24	4.87	4.95	0.63	4.57	0.57	0.06	3.88	4.05	0.75	3.89	0.67
49	1.0	6.2	0.80	2.98	0.8	2.57	1.28	4.83	1.14	2.97	1.04	2.59	0.81	5.34	0.76	2.97	0.71	2.58
50	9.4	1.2	15.86	3.36	14.9	3.55	8.01	7.38	8.80	8.25	8.45	8.36	10.20	6.17	10.5	7.26	10.21	7.27
51	1.1	0.8	2.05	0.29	1.9	0.26	0.67	0.72	1.68	0.38	1.71	0.40	0.69	0.74	1.70	0.26	1.71	0.26
52	1.7	2.7	0.90	2.99	0.8	2.75	2.20	1.55	1.01	2.15	0.955	2.07	1.91	2.19	0.77	2.87	0.71	2.69
53	0.1	0.0	3.11	3.93	2.9	3.72	0.07	0.24	1.36	6.31	1.26	5.93	0.08	0.14	1.63	5.50	1.56	5.32
54	0.7	7.1	0.00	0.03	0.0	0.03	0.89	7.56	0.01	0.27	0.00	0.19	1.16	7.13	0.00	0.12	0.003	0.09

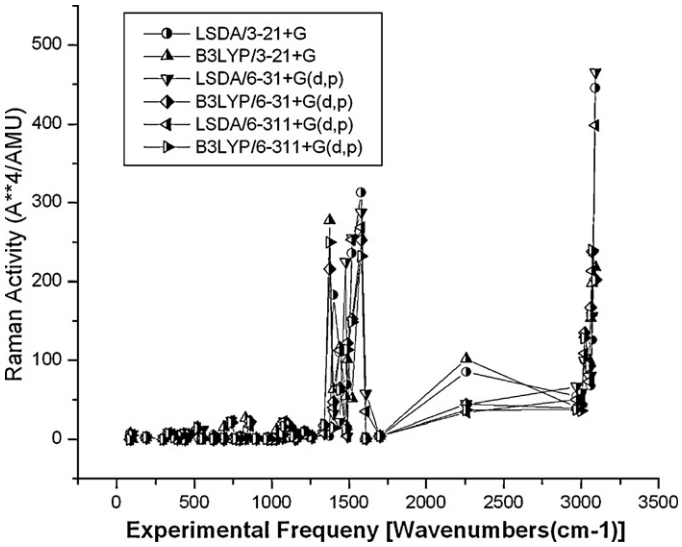

Fig. 8. Comparative graph of Raman activities by DFT [LSDA/B3LYP].

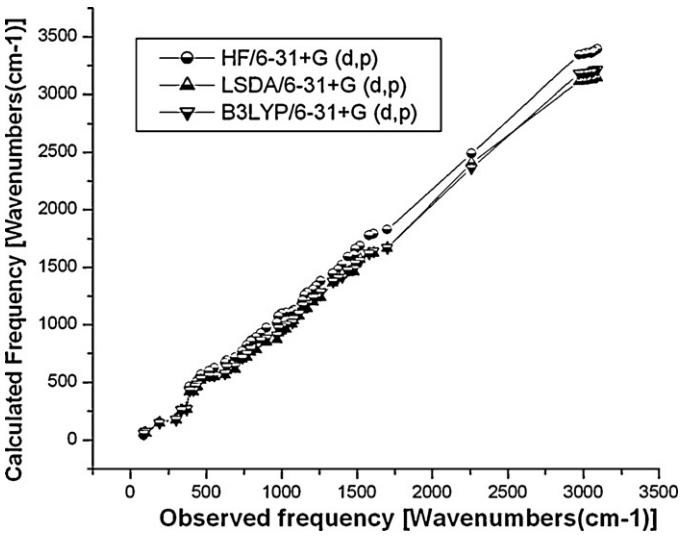

Fig. 9. Comparative graph of experimental and computed frequencies by HF and DFT [LSDA/B3LYP].

4.3. Computed vibrational frequency analysis

The comparative graph of calculated vibrational frequencies by DFT methods for ICANE is given in Fig. 9. From the figure it is found that the calculated frequencies by LSDA/3-21+G, LSDA/6-31+G(d,p) and B3LYP/6-31+G(d,p) basis set are closer to the experimental values [28,29]. The standard deviation (SD) calculation made between experimental and computed frequencies DFT for the title molecule presented in Table 4. According to the standard deviation the computed frequency deviation increase in going from HF/6-31+G(d,p) to B3LYP/6-31+G(d,p) to LSDA/6-31+G(d,p), for 3-21+G and 6311+G(d,p), from B3LYP to LSDA to HF. The biggest deviation ratio value is 2.967 for HF/6-31+G(d,p) and the smallest deviation ratio value is 0.773 for LSDA/6-31+G(d,p).

4.4. Ideal frequency estimation analysis

The ideal frequency estimation by DFT method is presented in Table 5. The frequency calculated by various basis set exactly coincide with experimentally observed values of FT-IR and FT-Raman without scaling while comparing the estimation of frequencies by different set of DFT method, the LSDA/3-21 basis set estimate accurately more number of frequency than other sets. The LSDA/3-21 basis set gives the frequencies accurately for C=C stretching, C–H in-plane bending, C–H out-of-plane bending and N=C=O stretching vibrations and also in B3LYP/6-31+G(d,p) basis set C=C and C–C stretching, C–H in-plane and out-of-plane bending, C–C–C in-plane bending and C–N in-plane bending vibrations are good consistent with the experimentally observed value.

4.5. Vibrational assignments

4.5.1. C–H vibrations

The substituted naphthalene gives rise to C–H stretching, C–H in-plane and C–H out-of-plane bending vibrations. The ICANE molecule gives rise to seven C–H stretching, seven C–H in-plane bending vibration and seven C–H out-plane bending vibration. Since ICANE is monosubstituted naphthalene ring system it has seven adjacent C–H moieties. The excepted seven C–H stretching vibrations corresponds to mode nos. 1–7. The unscaled and scaled vibration of 1–7 presented in Tables 6 and 7 respectively corresponds to stretching modes of C2–H16, C3–H17, C4–H11, C5–H13, C6–H12, C7–H15, C8–H14 unit. The vibrations of 1–7 assigned to aromatic C–H stretching in the region 3090–2970 cm^{-1} are in agreement with literature value [30,31]. Using LSDA/6-311+G(d,p), the C–H stretching vibrations are calculated 2970–3088 cm^{-1} which are in agreement with observed ones. These vibrations are not found to be affected due to the nature and position of the substituent, most of aromatic compounds have nearly four infrared peaks in the region 3080–3010 cm^{-1} due to ring C–H stretching bonds [32,33]. The C–H in-plane-bending vibrations usually occur in the region 1390–990 cm^{-1} and are very useful for characterization purposes [34]. It is noted from literature [35] that strong band around 1200 cm^{-1} appears due to valence oscillations in naphthalene. The C–H in plane bending vibrations assigned in the region 1170–1030 cm^{-1} (mode nos. 22–28) which is agreement with literatures [30–35].

The strong peaks below 960 cm^{-1}, clearly indicate its aromativity. Substitution patterns on the ring can be judged from

Table 4
Standard deviation of frequencies computed by HF/DFT (LSDA/B3LYP) at 3-21+G, 6-31+G(d,p) and 6-311+G(d,p) basis sets.

S. no.	Basic set levels	Total values	Average	Standard deviation average	Deviation ratio
	Experimental	65,210	1207.59		
1	HF/3-21+G	72,214	1337.29	99.362	
2	LSDA/3-21+G	66,093	1223.944	85.075	1.167
3	B3LYP/3-21+G	67,344	1247.111	81.029	1.049
4	HF/6-31+G(d,p)	70,751	1310.204	27.302	2.967
5	LSDA/6-31+G(d,p)	64,891	1201.682	35.318	0.773
6	B3LYP/6-31+G(d,p)	66,106	1224.185	32.200	1.096
7	HF/6-311+G(d,p)	70,436	1304.37	40.148	0.802
8	LSDA/6-311+G(d,p)	64,759	1199.241	36.874	1.088
9	B3LYP/6-311+G(d,p)	65,927	1220.87	34.452	1.070

Table 5
Ideal estimation of calculated frequencies by DFT (LSDA/3-21+G, LSDA/6-31/6-311+G(d,p) and B3LYP/3-21+G, B3LYP/6-31/6-311+G(d,p)) basis sets.

S. no.	Basis sets											
	LSDA/3-21+G	Assigned frequencies	LSDA/6-31+G(d,p)	Assigned frequencies	LSDA/6-311+G(d,p)	Assigned frequencies	B3LYP/3-21+G	Assigned frequencies	B3LYP/6-31+G(d,p)	Assigned frequencies	B3LYP/6-311+G(d,p)	Assigned frequencies
1	1602	(C=C) υ	1624	(C=C) υ	1230	(C–C) υ	1051	(C–H) δ	1670	(C=O) υ	1481	(C=C) υ
2	1587	(C=C) υ	1462	(C=C) υ	554	(C–N) δ	611	(–N=C=O) δ	1485	(C=C) υ	569	(C–N) δ
3	1532	(C=C) υ	1454	(C=C) υ			176	(–N=C=O) γ	1413	(C–C) υ		
4	1458	(C=C) υ	1239	(C–N) υ					1243	(C–C) υ		
5	1446	(–N=C=O) υs	1233	(C–C) υ					1185	(C–H) δ		
6	1419	(C–C) υ	1199	(C–C) υ					863	(C–H) γ		
7	1087	(C–H) δ	1128	(C–H) δ					802	(C–H) γ		
8	1012	(C–H) δ	546	(C–N) δ					789	(C–C–C–) δ		
9	1006	(C–H) γ	419	(C–C–C–) γ					631	(C–C–C–) δ		
10	986	(C–H) γ							558	(C–N) δ		
11	976	(C–H) γ										
12	858	(C–H) γ										
13	808	(C–H) γ										
14	641	(C–C–C–) δ										
15	172	(–N=C=O) γ										

the out-of-plane bending of the ring C–H bonds in the region 960–675 cm^{-1} and these bands are highly informative [36]. The strong peak at 1000 cm^{-1} is due to seven adjacent hydrogen atoms in the naphthalene ring confirm the mono-substituted nature of the ICANE compound. Mono-substituted benzene shows only a strong band between 700 and 770 cm^{-1} [37]. In the present work, the peaks at 1000, 980, 970, 900, 860, 830, 800 cm^{-1} in FT-IR and in FT-Raman confirms the C–H out-of-plane bending vibration which agrees with the above said literature values [36,37].

4.5.2. C=C vibrations

The ring stretching vibrations are very much important in the spectrum of naphthalene and its derivatives are highly characteristic of the aromatic ring itself. The C=C aromatic stretching, known as semicircle stretching, predicted 1602, 1624, 1616, 1619, 1637, 1630 in LSDA/3-21+G, LSDA/6-31/6-311+G(d,p) and B3LYP/3-21+G, B3LYP/6-31/6-311+G(d,p) basis set is in agreement with experimental observation of FT-IR spectra values at 1610 cm^{-1}. Socrates [38] mentioned that the presence of conjugate substituent such as C=C causes heavy doublet formation around the region 1625–1575 cm^{-1}.

Many ring vibrations are affected by the substitution to the aromatic ring of naphthalene. The six ring carbon atoms undergo coupled vibrations, called skeletal vibration and give a maximum of four bands in the region 1660–1420 cm^{-1} [39]. The bands between 1400–1650 cm^{-1} in benzene derivatives are assigned to C=C stretching modes [40,41] and in 1,5 dimethyl naphthalene the C=C stretching vibration are assigned at 1610–1500 cm^{-1} by Nagabalasubramanian et al. [5]. As predicted in the earlier references, in this title compound also there are five peaks 1610, 1580, 1520, 1490, 1480 cm^{-1} due to strong C=C stretching vibrations. The theoretically computed frequencies by LSDA/3-21+G, LSDA/6-31+G(d,p), B3LYP/6-31+G(d,p) and B3LYP/6-311+G(d,p) methods are assigned for C=C and C–C stretching vibrations approximately coincides with FT-IR and FT-Raman without scaling. In the present study the bands are assigned at 1440w, 1400s, 1375vs, 1340m, 1260, 1230 cm^{-1} to C–C stretching vibration [42]. Theoretically calculated C–C–C out-of-plane and in-plane bending modes have been found to consistent with recorded spectral values. The in-plane deformation vibration is higher frequencies than those out-of-plane vibrations. These assignments are in good agreement with the literature [5,8,39–41]. In this present work C–C–C-in-plane bending vibration assigned at 795, 770, 740, 690, 690 and 635 cm^{-1} and C–C–C-out-plane bending vibration assigned at 520, 465, 440, 430, 415 and 390 cm^{-1}.

4.5.3. C–N and C=N vibrations

The C–N stretching frequency is very difficult task since it falls in a complicated region of the vibrational spectrum, i.e., mixing of several bands are possible in this region [43] assigned C–N stretching absorption in the region 1386–1266 cm^{-1} for aromatic amines. The IR band appeared at 1260 cm^{-1} has been assigned to C–N stretching vibration. The in-plane and out-plane bending vibration assigned in this study are also supported by the literature [44–46]. In this title molecule the C–N in-plane bending vibration assigned at 635 cm^{-1}, the C–N out-of-plane bending vibration assigned at 370 cm^{-1} and the C–N twisting vibration occurs at 335 cm^{-1} in FT-IR. The theoretically computed value of CN vibrations may be mixing other vibrations.

4.5.4. C=O vibrations

The carbonyl stretching frequency has been most extensively studied by infrared spectroscopy [38]. This multiply bonded group is highly polar and therefore gives rise to an intense infrared absorption band. The carbon–oxygen double band is formed by π–π bonding between carbon and oxygen-intermolecular hydrogen

bonding, reduces the frequencies of the C=O stretching absorption to a greater degree than does inter molecular H bonding because of the different electro negative of C and O, the bonding are not equally distributed between two atoms. The loan pair of electrons on oxygen also determines the nature the carbonyl group. The most characteristic feature of carboxylic acids C=O band shows a strong absorption between 1700 and 1800 cm^{-1}. The C=O stretching bands of acids are considerably more intense than ketonic C=O stretching bands. The characteristic ketonic frequency C=O in the present study appears at 1700w cm^{-1} in FT-IR and FT-Raman spectrum (mode 9) which is calculated at 1703 cm^{-1} using B3LYP/6-311+G(d,p). This C=O vibration appears in the expected range shows that it is not much affected by other vibrations.

4.5.5. –N=C=O group vibrations

Due to the asymmetric stretching vibration of the –N=C=O group normally occurs at 2285–2250 cm^{-1} [47–49] which is slightly broader than the corresponding band observed for its derivatives. The symmetric stretching vibration band occurs at 1460–1340 cm^{-1}. In this study, the very strong band at 2260 cm^{-1} FT-IR spectrum (2260w cm^{-1} FT-Raman) and calculated band at 2260 cm^{-1} using B3LYP/6-31+G(d,p) are assigned to C=N stretching vibrations which have good correlation with literature data given above. The corresponding bending vibration of –N=C=O is observed in the region 640–605 cm^{-1} [49]. Accordingly, in this study a weak band is found at 635 cm^{-1}.

4.6. Thermodynamic properties

Several calculated thermodynamical parameters such as the Zero-Point Vibration Energies (ZPVE), the entropy, *S*, the molar capacity, *C*, at constant volume, rotational constants, rotational temperature and dipole moment have been presented in Table 1. The variations in the ZPVEs seem to be insignificant. The total energies are found to decrease with the increase of the basis set dimension. The changes in the total entropy of ICANE molecule at room temperature at different basis sets are only marginal.

On the basis of vibrational analysis at B3LYP/6-311+G(d,p) level, the standard statistical thermodynamic functions: standard heat capacity ($C^0_{p,m}$) standard entropy (S^0_m), and standard enthalpy changes (ΔH^0_m) for the title compounds were obtained from the theoretical harmonic frequencies and listed in Table 8.

From Table 8, it can be observed that these thermodynamic functions are increasing with temperature ranging from 100 to 700 K due to the fact that the molecular vibrational intensities increase with temperature [50]. The correlation equations between heat capacities, entropies, enthalpy changes and temperatures were fitted by quadratic formulas and the corresponding fitting factors (R^2) for these thermodynamic properties are 0.9987, 1.0000 and 0.9998, respectively. The corresponding fitting equations are as follows and the correlation graphics of that show in Figs. 10–12.

$$C^0_{p,m} = -2.1012 + 0.1557T - 6.4436 \times 10^{-5}T^2 \quad (R^2 = 0.9987)$$

$$S^0_m = 55.5077 + 0.1517T - 2.7877 \times 10^{-5}T^2 \quad (R^2 = 1.0000)$$

$$\Delta H^0_m = -0.3015 + 0.0079T + 5.3423 \times 10^{-5}T^2 (R^2 = 0.9998)$$

All the thermodynamic data supply helpful information for the further study on the ICANE. They can be used to compute the other thermodynamic energies according to relationships of thermodynamic functions and estimate directions of chemical reactions according to the second law of thermodynamics in Thermochemical field. Notice: all thermodynamic calculations were done in gas phase and they could not be used in solution.

4.7. HOMO–LUMO analysis

The total energy, energy gap and dipole moment have affect on the stability of a molecule. We have done optimization in order to investigate the energetic behavior and dipole moment of title compound in gas phase and two different solvents. The total energy, dipole moment and frontier molecular orbital energies have been calculated with B3LYP/6-311+G(d,p) level. Results obtained in solvent and gas phase are listed in Table 9.

The HOMO and the LUMO are very important parameters for chemical reaction. The HOMO is the orbital that primarily acts as

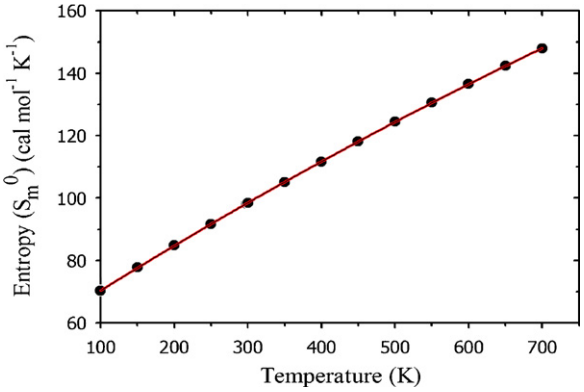

Fig. 11. Correlation graphic of entropy and temperature for 5-isocyanato-1,4-dihydronaphthalene molecule.

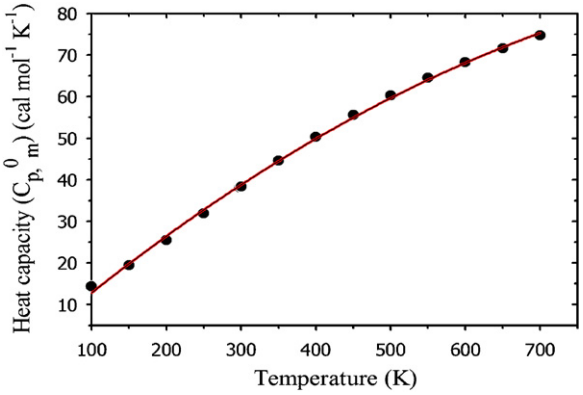

Fig. 10. Correlation graphic of heat capacity and temperature for 5-isocyanato-1,4-dihydronaphthalene molecule.

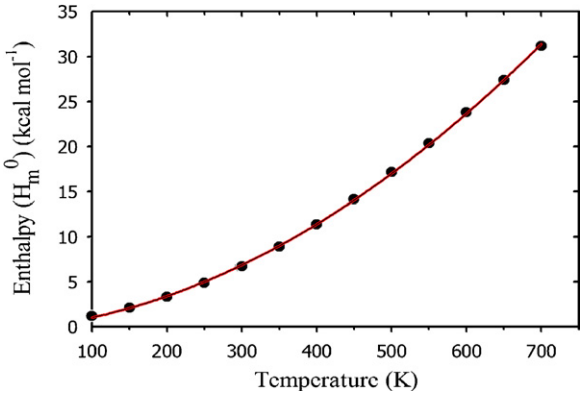

Fig. 12. Correlation graphic of enthalpy and temperature for 5-isocyanato-1,4-dihydronaphthalene molecule.

Table 6
Observed and HF/3-21/6-31/6-311+G(d,p), LSDA/3-21/6-31/6-311+G(d,p) and B3LYP/3-21/6-31/6-311+G(d,p) level calculated vibrational frequencies of isocyanic acid 1-naphthyl ester.

S. no.	Symmetry species C_S	Observed frequency		Calculated frequency									Vibrational assignments
		FT-IR	FT-Raman	HF			LSDA			B3LYP			
				3-21+G(d,p)	6-31+G(d,p)	6-311+G(d,p)	3-21+G(d,p)	6-31+G(d,p)	6-311+G(d,p)	3-21+G(d,p)	6-31+G(d,p)	6-311+G(d,p)	
1	A′	3090w		3070	3071	3072	3069	3072	3088	3072	3074	3102	C–H υ
2	A′		3070w	3063	3054	3054	3068	3072	3087	3067	3067	3095	C–H υ
3	A′	3060vs	3060vs	3053	3051	3050	3055	3061	3077	3060	3062	3090	C–H υ
4	A′	3050vs	3050	3048	3040	3039	3054	3058	3073	3054	3054	3082	C–H υ
5	A′	3020vw	3020w	3038	3037	3036	3002	2976	2977	3046	3050	2998	C–H υ
6	A′	3000vw		3032	3030	3029	2998	2974	2975	2978	2993	2993	C–H υ
7	A′	2970w		2959	2938	2938	2993	2969	2970	2972	2988	2988	C–H υ
8	A′	2260vs	2260w	2290	2252	2257	2289	2295	2299	2231	2260	2230	(–N=C=O) υ_{as}
9	A′	1700w	1700w	1667	1708	1675	1699	1740	1696	1663	1670	1703	C=O υ
10	A′	1610vs		1597	1619	1622	1602	1624	1597	1637	1612	1581	C=C υ
11	A′	1580vs	1580vs	1573	1607	1611	1587	1583	1590	1606	1595	1563	C=C υ
12	A′	1520vs	1520s	1500	1526	1527	1532	1535	1540	1557	1533	1502	C=C υ
13	A′	1490m		1474	1500	1501	1474	1497	1504	1529	1511	1482	C=C υ
14	A′	1480m		1457	1454	1457	1458	1462	1487	1508	1485	1481	C=C υ
15	A′	1440w		1437	1439	1441	1446	1454	1431	1407	1452	1424	N=C=O υ C–C υ
16	A′	1400s		1385	1377	1380	1419	1404	1407	1438	1413	1367	C–C υ
17	A′	1375vs		1354	1338	1411	1367	1383	1387	1396	1387	1354	C–C υ
18	A′	1340m		1313	1307	1307	1346	1335	1346	1305	1356	1326	C–C υ
19	A′	1260vs		1284	1247	1250	1262	1239	1270	1264	1264	1243	C–N υ
20	A′	1230s		1267	1210	1215	1242	1233	1230	1247	1243	1203	C–C υ
21	A′	1210m		1219	1180	1182	1221	1199	1231	1200	1215	1195	C–C υ
22	A′	1170vw	1170w	1201	1156	1159	1194	1194	1170	1189	1185	1148	C–H δ
23	A′	1150w		1178	1138	1141	1153	1187	1161	1159	1161	1140	C–H δ
24	A′		1140s	1152	1156	1154	1147	1128	1154	1149	1149	1132	C–H δ
25	A′		1115vw	1110	1094	1095	1129	1125	1102	1131	1128	1119	C–H δ
26	A′		1080vs	1087	1074	1070	1087	1083	1059	1107	1078	1070	C–H δ
27	A′	1070w		1062	1060	1058	1075	1049	1081	1051	1049	1043	C–H δ
28	A″	1030m	1030w	1053	1056	1003	1012	1006	1037	1051	1032	1029	C–H δ
29	A″	1000vs	1000s	1034	993	993	1006	985	1014	985	1014	1011	C–H γ
30	A″		980vw	1005	972	971	986	972	957	975	1001	999	C–H γ
31	A″	970vw		996	970	970	976	911	940	973	935	931	C–H γ
32	A‴	900vw	900vw	866	880	884	909	889	878	927	906	904	C–H γ
33	A″	860m	860vs	897	836	840	858	888	875	842	863	885	C–H γ
34	A″		830w	851	808	814	827	820	818	822	835	835	C–H γ
35	A″	800vs		829	781	789	808	819	808	801	802	824	C–H γ
36	A′		795m	805	773	775	787	798	784	784	789	811	C–C–C δ
37	A′	770vs	770vw	793	741	745	770	748	770	764	768	765	C–C–C δ
38	A′	740vw		740	733	711	741	732	725	708	731	733	C–C–C δ
39	A′	690vw	690s	678	682	692	686	641	679	674	657	664	C–C–C δ
40	A′	635w		647	625	636	641	625	638	630	631	658	C–C–C δ
41	A′		625vw	593	605	621	620	590	603	611	595	590	(–N=C=O) δ
42	A″	555s	555vs	585	566	568	551	546	554	553	558	569	C–N δ
43	A″	520vw	520s	546	540	543	541	516	527	537	532	528	C–C–C γ
44	A″	465w	465w	477	498	501	456	492	497	465	499	503	C–C–C γ
45	A″	440vw		474	466	470	450	444	443	464	459	450	C–C–C γ
46	A″		430vw	460	448	451	400	435	438	403	445	440	C–C–C γ
47	A″	415m	415m	408	420	423	378	419	434	390	411	408	C–C–C γ
48	A′	390w		398	417	422	360	398	395	363	409	402	C–C–C γ
49	A″	370w		400	402	403	394	397	386	399	390	385	(C=O) δ
50	A″	335w		351	374	374	341	374	374	343	373	375	(C–N) γ
51	A″	300s		261	262	264	267	261	255	272	261	258	(C–N) τ
52	A″	190s		231	217	218	172	227	219	176	218	215	(–N=C=O) γ
53	A″	100m		108	91	100	117	92	100	115	105	110	(–N=C=O) τ
54	A″	90m		59	55	49	81	91	82	83	82	73	

Table 7
Observed and HF/3-21/6-31/6-311+G(d,p), LSDA/3-21/6-31/6-311+G(d,p) and B3LYP/3-21/6-31/6-311+G(d,p) level calculated vibrational frequencies of isocyanic acid 1-naphthyl ester.

S. no.	Calculated frequency-unscaled								
	3-21+G	6-31+G(d,p)	6-311+G(d,p)	3-21+G	6-31+G(d,p)	6-311+G(d,p)	3-21+G	6-31+G(d,p)	6-311+G(d,p)
1	3392	3393	3372	3138	3141	3125	3217	3215	3198
2	3384	3375	3352	3137	3141	3124	3212	3208	3191
3	3373	3371	3348	3124	3130	3114	3204	3203	3186
4	3368	3359	3336	3123	3127	3110	3198	3195	3177
5	3357	3356	3333	3114	3120	3104	3190	3190	3173
6	3350	3348	3325	3110	3117	3102	3185	3184	3167
7	3344	3343	3320	3105	3112	3097	3179	3179	3162
8	2530	2488	2478	2374	2406	2397	2336	2364	2360
9	1794	1827	1819	1635	1665	1655	1645	1670	1661
10	1765	1789	1780	1602	1624	1616	1619	1637	1630
11	1738	1776	1768	1587	1619	1609	1589	1619	1611
12	1657	1686	1676	1532	1570	1559	1540	1556	1548
13	1629	1658	1648	1507	1531	1522	1512	1534	1528
14	1611	1607	1599	1458	1462	1451	1492	1485	1481
15	1588	1590	1582	1446	1454	1448	1473	1474	1468
16	1530	1522	1515	1419	1436	1424	1422	1413	1409
17	1458	1479	1468	1398	1414	1404	1381	1408	1396
18	1451	1444	1435	1376	1365	1362	1366	1377	1367
19	1419	1378	1372	1290	1239	1239	1324	1283	1281
20	1400	1338	1334	1270	1233	1230	1306	1243	1240
21	1347	1304	1298	1248	1199	1201	1257	1234	1232
22	1327	1277	1272	1221	1143	1141	1245	1185	1184
23	1302	1258	1253	1179	1136	1133	1214	1179	1175
24	1273	1210	1201	1173	1128	1126	1203	1167	1167
25	1227	1146	1139	1154	1077	1075	1184	1095	1092
26	1201	1125	1113	1087	1036	1033	1095	1047	1044
27	1173	1110	1101	1035	1004	1007	1051	1018	1018
28	1164	1106	1101	1012	963	966	1040	1002	1004
29	1142	1097	1090	1006	943	945	1031	984	986
30	1111	1074	1066	986	930	934	1021	972	975
31	1101	1016	1009	976	872	876	1019	908	908
32	1076	972	970	929	851	857	971	880	882
33	991	924	922	858	850	854	882	863	863
34	940	893	893	846	785	798	861	811	815
35	916	863	866	808	784	788	839	802	804
36	890	854	851	805	764	765	821	789	791
37	876	819	818	770	716	718	800	746	746
38	818	768	780	713	700	707	741	710	715
39	749	714	720	701	626	633	706	638	648
40	715	691	698	641	598	622	660	631	642
41	655	668	682	597	565	562	611	578	576
42	646	625	624	563	546	554	579	558	569
43	603	597	596	553	541	550	562	557	559
44	592	567	566	534	516	518	546	531	532
45	589	515	516	527	465	462	545	480	476
46	508	495	495	468	456	457	474	465	466
47	507	464	464	443	419	423	458	430	432
48	440	461	463	421	417	412	426	428	425
49	340	290	289	303	266	259	308	268	263
50	298	270	268	262	251	251	265	256	256
51	222	189	189	205	175	171	210	179	176
52	196	157	156	172	152	147	176	150	147
53	92	66	72	90	62	67	89	72	75
54	50	40	35	62	61	55	64	56	50

an electron donor and the LUMO is the orbital that largely acts as the electron acceptor, and the gap between HOMO and LUMO characterizes the molecular chemical stability. The energy gap between the HOMO and the LUMO molecular orbitals is a critical parameter in determining molecular electrical transport properties because it is a measure of electron conductivity. The energy values of HOMO are computed −6.18792, −6.17758 and −6.19690 eV and LUMO are −1.75733, −1.75025 and −1.77692 eV, and the energy gap values are 4.43059, 4.42733 and 4.41998 eV in DMSO, chloroform and gas phase for ICANE molecule, respectively. Lower value in the HOMO and LUMO energy gap explains the eventual charge transfer interactions taking place within the molecule. Surfaces for the frontier orbitals were drawn to understand the bonding scheme of present compound. We examine the four important molecular orbitals (MOs) for title molecule: the second highest and highest occupied MOs and the lowest and the second lowest unoccupied MOs which we denote HOMO−1, HOMO, LUMO and LUMO+1, respectively. These MOs for gas phase are outlined in Fig. 13. The positive phase is red and the negative one is green. According to Fig. 13, the HOMO of ICANE submits a charge density localized at all molecules expects of between benzene rings, but LUMO is characterized by a charge distribution all molecules expect of N atom and between benzene rings.

Direction of the dipole moment vector in a molecule depends on the centers of positive and negative charges. Dipole moments are strictly determined for neutral molecules. We can say that in going from the gas phase to the solvent phase, the dipole moment value increases (Table 9).

Table 8
Thermodynamic properties at different temperatures at the B3LYP/6-311+G(d,p) level for isocyanic acid 1-naphthyl ester molecule.

T (K)	$C^0_{p,m}$ (cal mol^{-1} K^{-1})	S^0_m (cal mol^{-1} K^{-1})	ΔH^0_m (kcal mol^{-1})
100	14.378	70.292	1.187
150	19.457	77.852	2.128
200	25.454	84.825	3.347
250	31.898	91.637	4.879
298.15	38.137	98.140	6.662
300	38.374	98.390	6.736
350	44.585	105.082	8.911
400	50.354	111.683	11.386
450	55.601	118.157	14.136
500	60.318	124.473	17.136
550	64.534	130.613	20.359
600	68.299	136.565	23.781
650	71.667	142.327	27.381
700	74.690	147.897	31.140

4.8. UV–vis spectra analysis

Molecules allow strong π–π* and σ–σ* transition in the UV–vis region with high extinction coefficients. Ultraviolet spectra analyses of ICANE have been researched by theoretical calculation. In order to understand electronic transitions of compound, TD-DFT calculations on electronic absorption spectra in gas phase and solvent (DMSO and chloroform) were performed. The calculated frontier orbital energies, absorption wavelengths (λ), oscillator strengths (*f*) and excitation energies (*E*) for gas phase and solvent (DMSO and chloroform) are illustrated in Table 10. The major contributions of the transitions were designated with the aid of Swizard program [51]. The visible absorption maxima of this molecule from calculations of the molecular orbital geometry show that correspond to the electron transition between frontier orbitals such as translation from HOMO to LUMO. As can be seen from

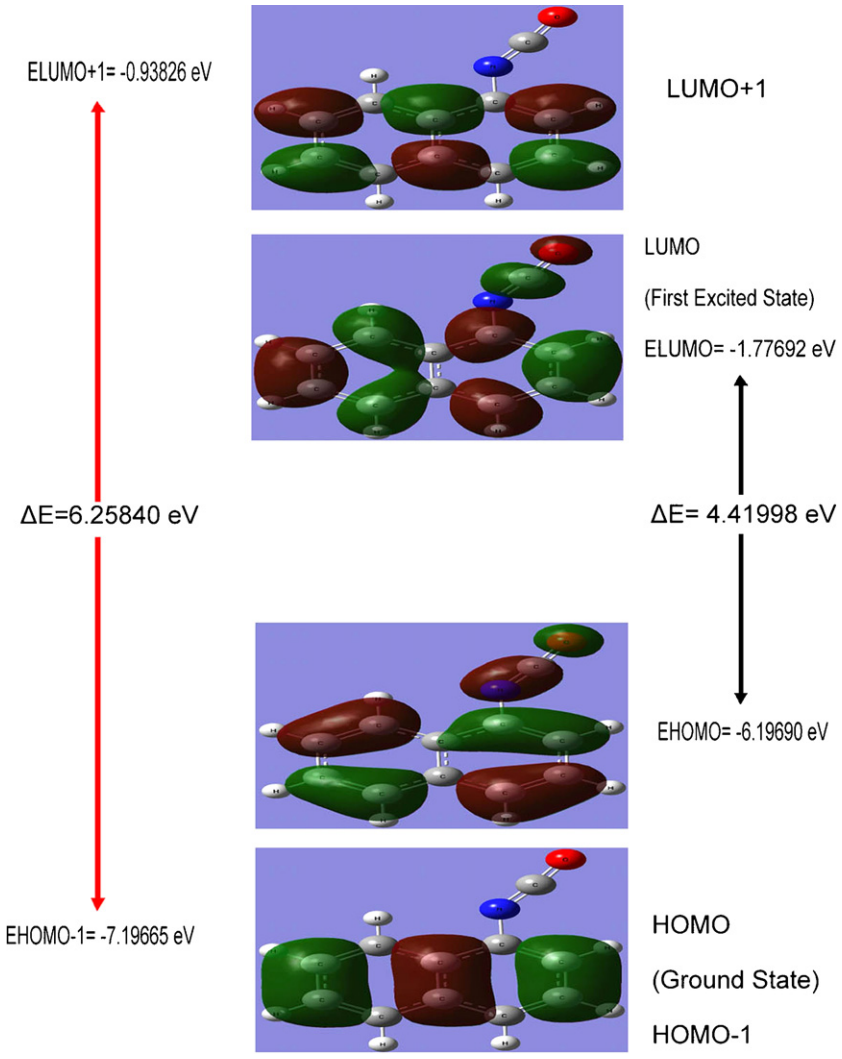

Fig. 13. The atomic orbital compositions of the frontier molecular orbital for 5-isocyanato-1,4-dihydronaphthalene molecule.

Table 9
Calculated energies values of isocyanic acid 1-naphthyl ester in gas and solvent (DMSO and chloroform) phase.

TD-DFT/B3LYP/6-311G+(d,p)	DMSO	Chloroform	Gas
E_{total} (Hartree)	−553.37865433	−553.37717357	−553.37175441
E_{HOMO} (eV)	−6.18792	−6.17758	−6.19690
E_{LUMO} (eV)	−1.75733	−1.75025	−1.77692
$\Delta E_{HOMO-LUMO\,gap}$ (eV)	4.43059	4.42733	4.41998
E_{HOMO-1} (eV)	−7.18250	−7.17107	−7.19665
E_{LUMO+1} (eV)	−0.90996	−0.90370	−0.93826
$\Delta E_{HOMO-1-LUMO+1\,gap}$ (eV)	6.27255	6.26738	6.25840
Dipole moment	3.0978	2.9642	2.5480

Table 10
Theoretical electronic absorption spectra of isocyanic acid 1-naphthyl ester (absorption wavelength λ (nm), excitation energies *E* (eV) and oscillator strengths (*f*)) using TD-DFT/B3LYP/6-311+G(d,p) method in gas and solvent (DMSO and chloroform) phase.

DMSO			Chloroform			Gas			Gas
λ (nm)	*E* (eV)	(*f*)	λ (nm)	*E* (eV)	(*f*)	λ (nm)	*E* (eV)	(*f*)	Major contribution[a]
308.35	4.0209	0.1920	308.76	4.0155	0.1946	305.63	4.0566	0.1398	H → L (95%)
286.87	4.3220	0.0045	287.11	4.3183	0.0046	287.37	4.3145	0.0034	H → L+1 (56%), H-1 → L (43%)
248.72	4.9849	0.0005	249.39	4.9715	0.0004	249.49	4.9695	0.0004	H → L+2 (93%)

[a] H: Homo, L: Lumo.

Table 9, the calculated absorption maxima values have been found to be 305.63, 287.37, 249.49 nm for gas phase, 308.35, 286.87, 248.72 nm for DMSO solution and 308.76, 287.11, 249.39 nm for chloroform solution at DFT/B3LYP/6-311+G(d,p) method. As can be seen, all calculations performed are very close. In view of calculated absorption spectra, the maximum absorption wavelength corresponds to the electronic transition from HOMO to LUMO with 95% contribution. This transition (H → L) is predicted as n–π* transition. The other transitions are predicted as π–π* transition The other wavelength, excitation energies, oscillator strength, calculated counterparts with major contributions and assignments can be seen in Table 10.

5. Conclusion

Attempt has been made in the present work for proper frequency assignments for the compound isocyanic acid 1-naphthyl ester from the FT-IR and FT-Raman spectra. The optimized structural parameter such as bond length, bond angle, dihedral angles, UV–vis spectral analysis, HOMO and LUMO energy are also calculated and are compared among HF and DFT (B3LYP and LSDA) methods. Comparison between the calculated vibrational frequencies and the experimental values indicate that FT-IR and FT-Raman spectra of the title compound well. The scaling factor used in this study made a reliable agreement between the calculated and experimental values. The C–C stretching, C–C–C in-plane bending, C–H stretching, in-plane and out-of-plane bending and C=C stretching (–N=C=O) asymmetric and symmetric stretching vibrational frequencies are observed well with the expected range compared to the literature values. The assignments made at higher level of theories with only reasonable deviations from the experimental values seem to be consistent. Various quantum chemical calculations help us to identify the structural and symmetry properties of the titled molecule. The excellent agreement of the calculated and observed vibrational spectra reveals the advantages of higher basis set for quantum chemical calculations. The calculated HOMO and LUMO energies show that charge transfer occurs within the molecule. The lowering of the HOMO–LUMO energy gap value has substantial influence on the intra molecular charge transfer and bioactivity of the molecule. The correlations between the statistical thermodynamics and temperature are also obtained. It is seen that the heat capacities, entropies and enthalpies increase with the increasing temperature owing to the intensities of the molecular vibrations increase with increasing temperature.

References

[1] V. Krishnakumar, N. Prabavathi, S. Muthunatesan, Spectrochim. Acta A 69 (2008) 528–533.
[2] S. Chandra, H. Saleem, N. Sundaraganesan, S. Sebastian, Spectrochim. Acta A 74 (2009) 704–713.
[3] J. Xavier, V. Balachandran, M. Arivazhagan, G. Ilango, Ind. J. Pure Appl. Phys. 48 (2010) 245–250.
[4] P. Das, E. Arunan, P.K. Das, Vib. Spectrosc. 47 (2008) 1–9.
[5] P.B. Nagabalasubramanian, S. Periandy, Spectrochim. Acta A 77 (2010) 1099–1107.
[6] M. Govindarajan, K. Ganasan, S. Periandy, M. Karabacak, Spectrochim. Acta A 79 (2011) 646–653.
[7] J. Karpagam, N. Sundaraganesan, S. Sebastian, S. Manoharan, M. Kurt, J. Raman Spectrosc. 41 (2010) 53–62.
[8] V. Krishnakumar, R. Mathammal, S. Muthunatesan, Spectrochim. Acta A 70 (2008) 210–216.
[9] J. Liebig, F. Wöhler, Ann. Phys. 20 (1830) 394.
[10] A. Baeyer, J. Liebigs, Ann. Chem. 114 (1860) 165.
[11] Gmelin, System Nr. 14 (1971) 327–366.
[12] M. Linhard, Z. Anorg. Allg. Chem. 239 (1938) 200.
[13] G.T. Fujimoto, M.E. Umstead, M.C. Lin, J. Chem. Phys. 65 (1982) 197.
[14] M. Zyrianov, T. Droz-Georget, A. Sanov, H. Reisler, J. Chem. Phys. 105 (1996) 8111.
[15] A. Senier, C. Walsh, J. Chem. Soc. 81 (1908) 290.
[16] W. Kern, H. Paul, W. Mehren, J. Makromol. Chem. Ges. 38 (1954) 1013.
[17] Z. Qui, Z. Fang, M. Cheng, D. Zhao, J. Shiyou Huagong Xueyuan Xuebao 11 (1999) 56.
[18] A.E.A. Werner, W.R. Fearon, J. Chem. Soc. 117 (1920) 1326.
[19] A.E.A. Werner, J. Gray, Sci. Proc. R. Dublin Soc. 24 (1947) 209.
[20] E. Hayek, Monatsh. Chem. 96 (1965) 517.
[21] Gaussion 03 Program, Gaussian Inc., Wallingford, CT, 2004.
[22] H.B. Schlegel, J. Comput. Chem. 3 (1982) 214.
[23] M.J. Frisch, A.B. Nielsen, A.J. Holder, Gauss View Users Manual, Gaussian Inc., Pittsburgh, PA, 2000.
[24] G.S. Jas, K. Kuczera, Chem. Phys. 214 (1997) 229–241.
[25] V. Krishnakumar, N. Prabavathi, S. Muthunatesan, Spectrochim. Acta A 68 (2007) 771–777.
[26] V. Krishnakumar, R. Mathammal, S. Muthunatesan, Spectrochim. Acta A 70 (2008) 201–209.
[27] A. Srivastava, V.B. Singh, Ind. J. Pure Appl. Phys. 45 (2007) 714–720.
[28] S. Ramalingam, S. Periandy, B. Narayanan, S. Mohan, Spectrochim. Acta 75A (2010) 84–92.
[29] P.D.S. Babu, S. Periandy, S. Mohan, S. Ramalingam, B.G. Jayaprakash, Spectrochim. Acta (2010).
[30] K. Raslogi, M.A. Plalfox, R.P. Tanwar, L. Mithal, Spectrochim. Acta A58 (2002) 1989.
[31] Y.R. Sharma, Elementary Organic Spectroscopy—Principles and Chemical Applications, S. Chande & Company, Ltd., New Delhi, 1994, pp. 92–93.
[32] F.B.S. Vogel, Text Book of Practical Organic Chemistry, 5th ed., Longman/Widely, New York, 1989.

[33] L.G. Wade (Ed.), Advanced Organic Chemistry, 4th ed., Wiley, New York, 1992, p. 723.
[34] M. Pagannone, B. Formari, G. Mattel, Spectrochim. Acta 43A (1986) 621.
[35] A.R. Prabakaran, S. Mohan, Indian J. Phys. 63B (1989) 468–473.
[36] P.S. Kalsi, Spectroscopy of Organic Compounds, Wiley Eastern Limited, New Delhi, 1993, pp. 116–117.
[37] J. Mohan, Organic Spectroscopy—Principle and Applications, 2nd ed., Narosa Publishing House, New Delhi, 2004, pp. 30–32.
[38] G. Socrates, Infrared and Raman Characteristic Frequencies, 3rd ed., John Wiley & Sons Ltd., Chichester, 2001.
[39] V.R. Dani, Organic Spectroscopy, Tata-MacGraw Hill Publishing Company, New Delhi, 1995, p. 139.
[40] D.N. Sathyanarayana, Vibrational Spectroscopy Theory and Application, New Age International Publishers, New Delhi, 2004.
[41] A.U. Rani, N. Sundaraganesan, M. Kurt, M. Cinar, M. Karabacak, Spectrochim. Acta A 75 (2010) 1523–1529.
[42] M. Govindarajan, K. Ganesan, S. Periandy, S. Mohan, Spectrochim. Acta Part A 76 (2010) 12–21.
[43] M. Silverstein, G.C. Basseler, C. Morill, Spectrometric Identification of Organic Compounds, Wiley, New York, 1981.
[44] K.C. Medhi, R. Barman, M.K. Sharma, Indian J. Phys. 68B (2) (1994) 189.
[45] B. Smith, Infrared Spectral Interpretation: A Systematic Approach, CRC Press, Washington, DC, 1999.
[46] M. Arivashagan, V. Krishnakumar, R.J. Xavier, G. Ilango, V. Balachandran, Spectrochim. Acta A 72 (2009) 941–946.
[47] E.A. Nicol, et al., Spectrochim. Acta 30 (1974) 1717.
[48] G.D. Caldow, H.W. Thomson, Spectrochim. Acta 13 (1958) 212.
[49] R.P. Hirschmann, et al., Spectrochim. Acta A 30 (1974) 1293.
[50] J. Bevan Ott, J. Boerio-Goates, Calculations from Statistical Thermodynamics, Academic Press, 2000.
[51] S.I. Gorelsky, SWizard Program Revision 4.5, University of Ottawa, Ottawa, Canada, 2010, http://www.sg.chem.net/.